A comparison of the spatial patterns of β-amyloid (Aβ) deposits in five neurodegenerative disorders

Richard A. Armstrong

Vision Sciences, Aston University, Birmingham, United Kingdom

Abstract

Alzheimer's disease neuropathologic change (ADNC) in the form of β-amyloid (Aβ) deposits is important not only in the pathogenesis of Alzheimer's disease (AD) and Down's syndrome (DS) but also as a 'co-pathology' in disorders such as dementia with Lewy bodies (DLB), corticobasal degeneration (CBD), and chronic traumatic encephalopathy (CTE). To compare cortical and hippocampal degeneration in different disorders, the spatial patterns of the diffuse, primitive, and classic Aβ deposits were studied in regions of frontal and temporal cortex in five neurodegenerative disorders, viz. AD, DS, DLB, CBD, and CTE using spatial pattern analysis. In all disorders, the Aβ deposits were clustered and in a proportion of brain regions, the clusters were regularly distributed parallel to the tissue boundary. Cluster dimensions in the cortex, measured parallel to the pia mater, were frequently in the range 400-800 μm suggesting a spatial association with the cortico-cortical pathways. Differences were also observed among disorders, the diffuse Aβ deposits being more frequently distributed in regular clusters in AD while cluster sizes of the diffuse and primitive deposits were significantly smaller in CTE. The data suggest considerable similarities in the spatial patterns of Aβ deposits in different disorders, regardless of the clinical or pathological setting, which suggests that the spread of Aβ via neuro-anatomical pathways may be common to several disorders.

Key words: *Alzheimer's disease neuropathologic change (ADNC), β-amyloid (Aβ), pathogenic spread.*

Introduction

Alzheimer's disease neuropathologic change (ADNC) in the form of β-amyloid (Aβ) deposits [26,35] occurs in a variety of neurodegenerative disorders. Aβ is a 'signature' pathological lesion of Alzheimer's disease (AD) [19] and also plays a significant role in the pathology of Down's syndrome (DS) [19,30,36,45]. In addition, Aβ deposits have been recorded as a 'co-pathology' in many other neurode-generative disorders including dementia with Lewy bodies (DLB) [6], Parkinson's disease (PD) [38], Pick's disease (PiD) [38], corticobasal degeneration (CBD) [38], amyotrophic lateral sclerosis (ALS) [22], progressive supranuclear palsy (PSP) [38], and chronic traumatic encephalopathy (CTE) [31].

Aβ peptides are generated via β- and γ-secretase cleaving of amyloid precursor protein (APP) resulting in the formation of aggregated protein deposits [21,25]. A number of distinct types of Aβ deposit have

Communicating author

Dr Phil. Richard A. Armstrong, Vision Sciences, Aston University, Birmingham B4 7ET, United Kingdom, phone: 0121-204-4102, fax: 0121-204-4048, e-mail: R.A.Armstrong@aston.ac.uk

been described but the majority are classifiable into three morphological groups [17]. First, diffuse deposits are 10-200 µm in diameter, irregular in shape with diffuse boundaries, and are lightly immunolabeled with antibodies raised against Aβ. Second, primitive deposits are 20-60 µm in diameter, well demarcated, more symmetrical in shape, and more strongly immunolabeled. Third, classic deposits are 20-100 µm and comprise a distinct central 'core' surrounded by a 'corona' of dystrophic neurites (DN). Previous studies suggest that in the cerebral cortex, Aβ deposits are distributed with a degree of clustering of deposits regularly distributed parallel to the pia mater [3]. Aβ deposits may occur in discreet clusters but more frequently there is a continuous variation in density parallel to the tissue boundary with a succession of relatively dense areas interspersed with less dense areas [3]. This pattern suggests a spatial association between the Aβ deposits and the degeneration of neuro-anatomical pathways such as the cortico-cortical projections [16,23,37]. This spatial association may also be the result of the hypothesized 'prion-like' spread of Aβ via neuro-anatomical connections [20,43]. Hence, previous studies of Creutzfeldt-Jakob disease (CJD), in which propagation of prion protein (PrP^{sc}) along neuro-anatomical pathways is well documented [10-12], deposits of PrP^{sc} are also clustered in the cerebral cortex, the clusters being regularly distributed parallel to the pia mater similar to the Aβ deposits in AD [7]. Hence, the presence of regularly distributed clusters of a pathology may be a marker of the spread of pathogenic proteins such as Aβ.

This study compared the spatial patterns of the Aβ deposits in five neurodegenerative disorders, viz. AD, DS, DLB, CBD, and CTE in which the Aβ peptide occurs in different clinical and pathological settings. Hence, Aβ is the primary pathological change in AD and DS, a co-pathology in CBD, whereas in DLB it may represent a more intermediate condition. In addition, the disorders vary in their molecular pathology. Hence, AD, CBD, and CTE are tauopathies in which the deposition of abnormal forms of the microtubule-associated protein (MAP), tau in the form of neurofibrillary tangles (NFT) is a defining feature [29]. By contrast, DLB is a synucleinopathy in which the synaptic protein α-synuclein is deposited in association with Lewy bodies (LB) [41]. In DS, Aβ results from triplication of the *APP* gene [39] while in CTE, Aβ deposition may be the result of repetitive brain injury [18,28,42]. The principle objectives were to compare the spatial patterns of Aβ deposits among disorders and to determine whether there was evidence of the pathogenic spread of Aβ especially between adjacent cortical gyri such as the lateral occipito-temporal gyrus (LOT) and parahippocampal gyrus (PHG).

Material and methods

Cases

Demographic data and diagnostic criteria for the five disorders are listed in Table I. Informed consent was given for the removal of all brain tissue according to the 1996 Declaration of Helsinki (as modified Edinburgh 2000). Case material for AD, DS, DLB, and CBD, in the form of microscope slides, was obtained from the Brain Bank, Department of Neuropathology, Institute of Psychiatry, King's College, London, UK. The primary criterion for the selection of the CBD, DLB, and CTE cases was the presence of suf-

Table I. Summary of demographic details, signature pathology, associated pathology, and diagnostic criteria in the disorders studied (*n* is the number of cases studied in each disorder)

Disorder, *n*	Mean age, years (SD)	M : F	Signature lesion	Additional pathology	Diagnostic criteria
AD, 10	78.2 (8.3)	3 : 7	Aβ deposits	NFT, GVC, EN	NINCDS/ADRDA/CERAD
CBD, 4	62.5 (8.01)	2 : 2	NFT	AP, GI, EN	NIH-ORD
CTE, 6	71.6 (8.2)	6 : 0	NFT	DN, DLG	McKee *et al.* [32]
DLB, 8	71.5 (3.40)	8 : 0	LB	LN, LG	CDLB
DS, 11	40.7 (4.03)	6 : 5	Aβ deposits	NFT	By karyotype

Disorders: AD – Alzheimer's disease, DS – Down's syndrome, CTE – chronic traumatic encephalopathy, DLB – dementia with Lewy bodies, CBD – corticobasal degeneration
Neuropathology: Aβ – β-amyloid, AP – astrocytic plaques, DN – dystrophic neurites, DLG – dot-like grains, EN – enlarged neurons, GI – glial inclusions, GVC – granulovacuolar change, LB – Lewy bodies, LG – Lewy grains, LN – Lewy neurites, NFT – neurofibrillary tangles
Diagnostic criteria: 'National Institute of Neurological and Communicative Disorders and Stroke and the Alzheimer Disease and Related Disorders Association' (NINCDS/ADRDA) [44], 'Consortium to Establish a Registry of Alzheimer Disease' (CERAD) criteria [34]; National Institute of Health-Office of rare disorders (NIH-ORD); 'Consortium on Dementia with Lewy bodies' (CDLB)' [33]
M – male, F – female, SD – standard deviation

Richard A. Armstrong

ficient densities of Aβ deposits consistent with the presence of ADNC [26,35]. By contrast, because of its scarcity, case material for CTE was obtained from Boston University's CTE center (VA-BU-CLF Brain Bank) as a series of scanned microscope images (Aperio Image-Scope Software, Leica Biosystems Inc. Buffalo Grove, IL, USA) [9]. All individuals with CTE had played American football, career durations being in the range of 11-24 years. In addition, all patients had suffered at least one traumatic episode resulting in concussion, some with accompanying loss of consciousness, the majority of cases having experienced multiple episodes of trauma during their careers. To determine whether the scanning of CTE slides affected the assessment of the spatial pattern compared with original microscope slides, a random sample of regions from the AD cases were studied both from microscope slides and from scanned images, no differences in the spatial pattern being detected.

Histological methods

Blocks of frontal (level of genu of corpus callosum) and temporal cortex (at the level of the lateral geniculate nucleus) were taken from each case to study the superior frontal gyrus (SFG) (B8), lateral-occipito-temporal gyrus (LOT) (B36), parahippocampal gyrus (PHG) (B28), and hippocampus (HC), regions which have high densities of Aβ deposits in the disorders studied [3]. Tissue was fixed in 10% phosphate buffered formal-saline and embedded in paraffin wax. 7 μm coronal sections were immuno-labeled with two rabbit polyclonal antibodies which recognize $Aβ_{1-42}$: (1) Gift of Professor BH Anderton, Institute of Psychiatry, King's College London, UK [40] and (2) END Millipore Billerica, MA, USA, (1 : 2000) [42] and counterstained with hematoxylin/eosin (H/E). Both antibodies identify $Aβ_{1-42}$ and clearly revealed the diffuse, primitive, and classic subtypes of Aβ deposit which were identified in the sections using previously defined criteria [17].

Morphometric methods

In each region where a sufficient density of an Aβ deposit was present (at least 20 deposits along a transect), spatial distribution was studied along each gyrus or CA sectors of the hippocampus using 200 × 1000 μm contiguous sample fields; the short dimension of the field being aligned with the surface of the tissue boundary [1]. In the cerebral cortex, the sample fields were aligned with the surface of the pia mater, the longer dimension of the field including layers I, II, and most of layer III; regions which contain the highest densities of Aβ deposits in the various disorders [3]. The sample fields were extended from the PHG/subiculum into the HC, the fields aligned first, with the alveus to sample sectors CA1 to CA3 and second, using a guideline marked on the slide and which ceased approximately 400 μm from the dentate gyrus fascia, to sample sector CA4.

The number of diffuse, primitive, and classic Aβ deposits was counted in each sample field. AD, DS, DLB, and CBD were examined using microscope slides at a magnification of ×100 using a micrometer grid with grid lines at intervals of 10 μm to define the sample field. By contrast, CTE was examined using the scanned images at ×100, the sample fields arranged contiguously and superimposed over the image using either the draw or rectangle options. The short edge of the sample field was orientated parallel with the pia mater and aligned with guidelines also marked on the section. Between 32 and 64 sample fields were necessary to study each gyrus or CA sector depending on its length. The diffuse and primitive deposits were present in most brain regions studied but the classic deposits were present in a more restricted number of regions. Hence, there are different numbers of analyses of the diffuse, primitive, and classic Aβ deposits depending on their relative frequency.

To estimate the intra- and inter-observer variability in counts of Aβ deposits, five images selected at random were counted twice by the same observer one month apart and also by a second observer. Count-recount variability was tested using the 'method of agreement' described by Bland and Altman [13]. The essential feature of the Bland and Altman method is that for a particular histological feature, the difference between the two counts are subtracted for each case. The mean of these differences is known as the degree of 'bias' or 'agreement' and the standard deviation (SD) of the mean can be used to calculate the 'limits of agreement' in which it would be expected that 95% of the differences between two successive counts would fall. For example, there was a good agreement between successive counts made by the same observer (intra-observer variability) of the diffuse Aβ deposits in Sector CA1 in a case of CTE. The mean difference between the two counts of the

diffuse deposits, averaged over the 32 sample fields was 0.08 lesions per 200 × 1000 mm sample field (SD = 0.48, limits of agreement −0.87-1.02. There was less agreement between different observers (inter-observer variability) with a mean difference of 0.39 (SD = 0.48, limits of agreement −0.95 to +1.74. Similar results were obtained for the remaining four images.

Data analysis

The data were analyzed by spatial pattern analysis [2]; a method which uses the variance/mean (V/M) ratio as a measure of non-randomness and determines whether the deposits were distributed randomly (V/M = 1), regularly (V/M < 1) or in clusters (V/M > 1) along the strip of cortex parallel to the pia mater. To perform the analysis, the V/M ratio is calculated from the data at various field sizes, e.g., 200 × 1000 μm (the original field size) and then at 400 × 1000 μm, 800 × 1000 μm etc., up to a size limited by the length of cortex sampled. Data for the larger field sizes are obtained by adding together successively the densities of deposits in adjacent sample fields. The V/M ratio is plotted against the increasing field size to reveal the spatial pattern. If the deposits are clustered, then the analysis indicates whether the clusters themselves are randomly or regularly distributed and provides an estimate of

the mean dimension of the clusters in a plane parallel to the pia mater. Regularly spaced clusters are indicated by the V/M ratio increasing to a peak before declining at larger field sizes, the location of the peak corresponding to the mean dimension of the clusters. The frequency of cortical regions in which the size of regularly distributed clusters of deposits were in the range 400-800 μm, approximating to the dimension of the columns of neurons forming the cortico-cortical connections, was also determined [23]. Comparisons were made of the frequencies of different types of spatial pattern of the Aβ deposits: (1) among deposit types within a disorder, (2) among disorders, and (3) the proportion of regular clusters 400-800 μm in diameter using χ^2 contingency table tests. Mean cluster sizes of Aβ deposits in different regions were compared using 1-way analysis of variance (ANOVA) followed by the Tukey 'honestly significant difference' (THSD) *post-hoc* test.

Results

Figures 1-3 show variations in the density of Aβ deposits parallel to the pia mater in regions of the cerebral cortex in different disorders. Figure 1 shows the distribution of Aβ deposits in a case of AD, with the approximate positions of the clusters indicated, a number of clusters of deposits being evident main-
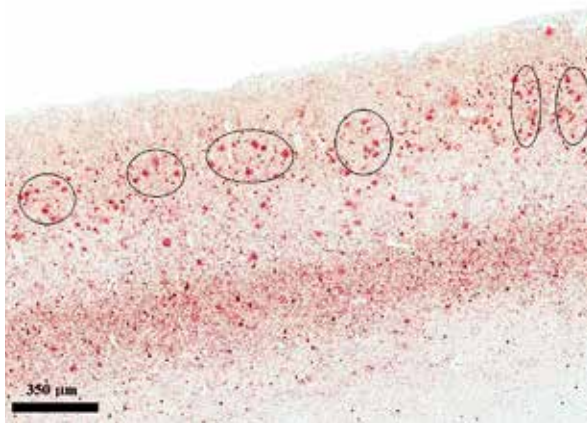

Fig. 1. Distribution of β-amyloid (Aβ) deposits along the superior frontal cortex in a case of Alzheimer's disease. The approximate location of clusters of deposits along the cortex parallel to the pia mater mainly in the upper cortical layers are circled (Aβ immunostaining, H/E).
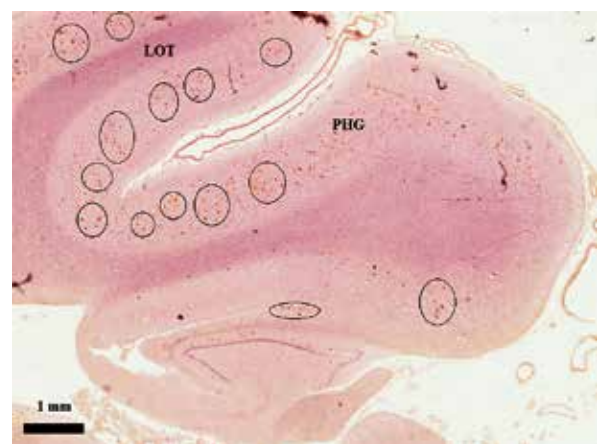

Fig. 2. Distribution of β-amyloid (Aβ) deposits along the lateral occipito-temporal gyrus (LOT) and parahippocampal gyrus (PHG) in a case of dementia with Lewy bodies. Clusters of deposits (approximate location circled) are present along the gyri affecting all layers (Aβ immunostaining, H/E).
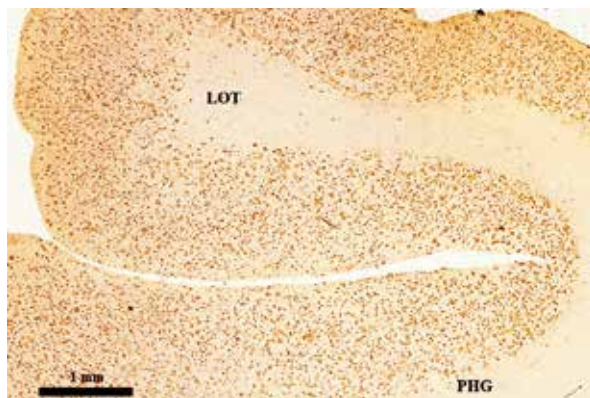
Fig. 3. Distribution of β-amyloid (Aβ) deposits along the lateral occipito-temporal gyrus (LOT) and parahippocampal gyrus (PHG) in a case of Down's syndrome. Clustering of deposits is absent and a more continuous distribution is present affecting all layers (Aβ immunostaining, H/E).
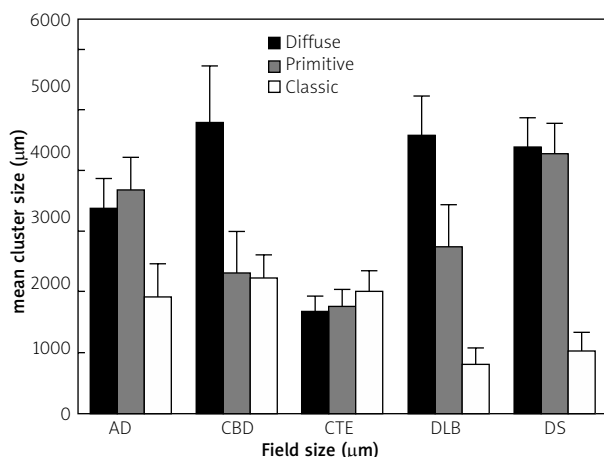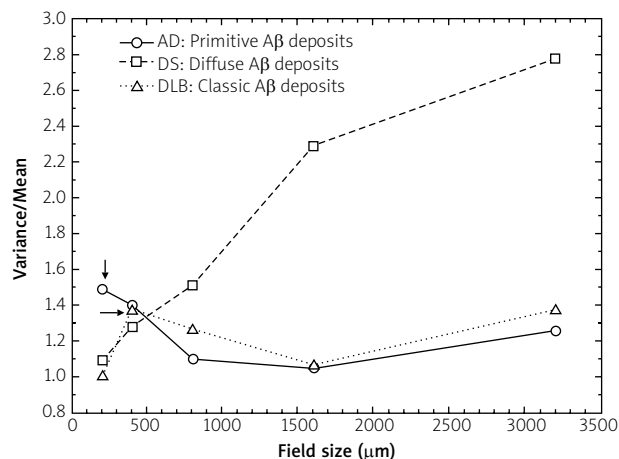

Fig. 4. Pattern analysis plots showing examples of the spatial patterns exhibited by β-amyloid deposits: AD – Alzheimer's disease, DS – Down's syndrome, DLB – dementia with Lewy bodies. Significance of V/M peaks, arrows indicate $p < 0.01$.

Fig. 5. Mean cluster size of the β-amyloid (Aβ) deposits in Alzheimer's disease (AD), Down's syndrome (DS), dementia with Lewy bodies (DLB), corticobasal degeneration (CBD), and chronic traumatic encephalopathy (CTE). Analysis of variance (ANOVA) (one-way): diffuse deposits F = 6.00, $p < 0.001$, *post-hoc* CTE < CBD/DS/DLB; primitive deposits F = 3.85, $p < 0.001$ *post-hoc* CTE < AD/DS; classic deposits F = 1.44, $p > 0.05$).

ly in the upper cortex and with a degree of regular spacing along the cortex. Figure 2 shows clustering of Aβ deposits in the PHG and LOT in a case of DLB with significantly fewer deposits in the HC while in Figure 3, the Aβ deposits are more continuously distributed along the PHG and LOT in a case of DS,

and where it is virtually impossible to detect specific clusters.

Examples of the spatial pattern analysis are shown in Figure 4. First in AD, the primitive Aβ deposits in the PHG exhibited a V/M peak at a field size of 200 μm indicating a regular distribution of clusters of deposits 200 μm in diameter parallel to the pia mater. Second in DS, the diffuse deposits in the PHG exhibited an increase in V/M with field size without reaching a peak suggesting clustering of deposits on a larger scale. Third in DLB, the classic deposits in the PHG exhibited a V/M peak at a field size of 400 μm suggesting a regular distribution of clusters of deposits 400 μm in diameter.

The frequencies of the various spatial patterns of Aβ deposits summed over all cortical and hippocampal regions for each disorder are shown in Table II. The data suggested first, clustering of Aβ deposits was the most frequent spatial pattern present in all disorders, uniform or random distributions being rare. Second, in a significant proportion of regions, the clusters of Aβ deposits were regularly distributed parallel to the pia mater or alveus, this spatial pattern was present in all disorders varying in frequency from 63% of regions in AD to 39% in DS. Third, with the exception of CBD ($\chi^2 = 7.17$, 6 DF, $p > 0.05$) and CTE ($\chi^2 = 2.59$, 6 DF, $p > 0.05$), there were significant differences in spatial pattern exhibited by the three deposit subtypes, large-scale clustering

Table II. Spatial patterns of the diffuse (D), primitive (P), and classic (C) β-amyloid (Aβ) deposits in the cortex and hippocampus (HC) in five neurodegenerative disorders (AD – Alzheimer's disease, DS – Down's syndrome, DLB – dementia with Lewy bodies, CBD – corticobasal degeneration, CTE – chronic traumatic encephalopathy); n – total number of brain regions sampled, R – random distribution, Reg – regular or uniform distribution. Data represent the number of brain areas in which a specific type of spatial pattern is present. Data in parentheses in column 7 represent the number of brain areas in which regularly spaced clusters were present within the size range 400-800 μm

Disorder	Region	Aβ type	n	R	Reg	Regular clusters (200–6400 μm)	Large clusters (> 6400 μm)
AD	Cortex	D	25	0	0	17 (8)	8
	HC	D	5	0	0	3 (1)	2
	Cortex	P	26	0	0	12 (6)	14
	HC	P	5	0	0	3 (2)	2
	Cortex	C	14	0	2	11 (10)	1
	HC	C	4	0	1	2 (0)	1
CBD	Cortex	D	7	2	1	1 (0)	3
	HC	D	1	0	0	0	1
	Cortex	P	5	1	0	3 (2)	1
	HC	P	1	0	0	1 (0)	0
	Cortex	C	5	0	0	3 (2)	2
	HC	C	1	0	0	1 (0)	0
CTE	Cortex	D	19	2	1	10 (4)	6
	HC	D	7	0	0	3 (1)	4
	Cortex	P	14	0	2	8 (4)	4
	HC	P	10	0	0	4 (3)	6
	Cortex	C	10	0	0	6 (2)	4
	HC	C	6	2	1	0	3
DLB	Cortex	D	13	0	0	3 (4)	10
	HC	D	4	0	0	2 (0)	2
	Cortex	P	10	0	1	6 (3)	3
	HC	P	4	0	0	2 (1)	2
	Cortex	C	10	1	1	8 (6)	0
	HC	C	3	0	0	2 (1)	1
DS	Cortex	D	13	0	0	3 (2)	10
	HC	D	11	0	0	4 (1)	7
	Cortex	P	12	1	0	5 (2)	6
	HC	P	10	0	0	3 (1)	7
	Cortex	C	10	2	3	5 (3)	0
	HC	C	5	0	0	4 (2)	1

Comparison of spatial patterns (χ^2 contingency tables):

(1) Between cortex and HC: AD diffuse deposits $\chi^2 = 0.03$ (1DF, $p > 0.05$), primitive deposits $\chi^2 = 0.06$ (1DF, $p > 0.05$), classic deposits $\chi^2 = 1.45$ (1DF, $p > 0.05$); CTE diffuse deposits $\chi^2 = 2.07$ (3DF, $p > 0.05$), primitive deposits $\chi^2 = 3.15$ (2DF, $p > 0.05$), classic deposits $\chi^2 = 8.68$ (3DF, $p < 0.05$); DLB diffuse deposits $\chi^2 = 0.16$ (1DF, $p > 0.05$), primitive deposits $\chi^2 = 0.77$ (2DF, $p > 0.05$), classic deposits $\chi^2 = 3.99$ (3DF, $p > 0.05$); DS diffuse deposits $\chi^2 = 0.07$ (1DF, $p > 0.05$), primitive deposits $\chi^2 = 1.41$ (2DF, $p > 0.05$), classic deposits $\chi^2 = 5.00$ (3DF, $p > 0.05$)

(1) Among deposit types within each disorder totaled over all regions: AD $\chi^2 = 17.12$ (4DF, $p < 0.05$), DS $\chi^2 = 25.80$ (6DF, $p < 0.001$), DLB $\chi^2 = 17.34$ (6DF, $p < 0.05$), CBD $\chi^2 = 7.17$ (6DF, $p > 0.05$), CTE $\chi^2 = 2.59$ (6DF, $p > 0.05$)

(2) Among disorders totaled over all regions: diffuse deposits $\chi^2 = 33.14$ (12DF, $p < 0.001$), primitive deposits $\chi^2 = 16.83$ (12DF, $p > 0.05$), classic deposits $\chi^2 = 15.70$ (12DF, $p > 0.05$)

(3) Proportion of regular distributed clusters 400-800 mm in diameter among disorders: diffuse deposits $\chi^2 = 4.23$ (4DF, $p > 0.05$), primitive deposits $\chi^2 = 2.41$ (4DF, $p > 0.05$), classic deposits $\chi^2 = 6.18$ (4DF, $p > 0.05$)

of classic deposits being less frequently observed when compared to the diffuse and primitive deposits. Fourth, the primitive deposits (χ^2 = 16.83, 12 DF, p > 0.05) and classic deposits (χ^2 = 15.70, 12 DF, p < 0.05) exhibited no significant differences in spatial pattern among disorders. Fifth, the spatial patterns of the diffuse Aβ deposits varied among disorders (χ^2 = 33.14, 12 DF, p < 0.001), a greater proportion of brain regions in AD exhibiting regularly distributed clusters compared with the other disorders. Sixth, there were no significant differences among disorders in the proportions of regions exhibiting a regular pattern of clustering in which the diffuse (χ^2 = 4.23, 4 DF, p < 0.05), primitive (χ^2 = 2.41, 4 DF, p < 0.05), and classic (χ^2 = 6.18, 4 DF, p < 0.05) deposit clusters were in the range 400-800 mm.

A comparison of mean cluster sizes of the Aβ deposit in each disorder is shown in Figure 5. The data suggest: (1) a significant difference in cluster size of the diffuse deposits (F = 6.00, p < 0.001), cluster sizes being significantly smaller in CTE than in CBD, DLB and DS, (2) a significant difference in the cluster size of the primitive deposits (F = 3.85, p < 0.01), cluster sizes being significantly less in CTE compared with AD and DS, and (3) no significant differences in the cluster size of the classic deposits among disorders (F = 1.44, p > 0.05).

Discussion

A degree of intra-and inter-observer variability in the counts of Aβ deposits was detected, the inter-observer variability being consistently greater than intra-observer variability. The degree of consistency detected was comparable to that previously reported for counting NFT but superior to that when estimating surviving neuronal perikarya or the degree of vacuolation in fronto-temporal lobar degeneration (FTLD) [8]. In neither case did the variations in counts alter conclusions regarding the spatial pattern of the Aβ deposits.

The Aβ deposits commonly exhibited two types of spatial pattern: (1) regularly distributed clusters of deposits 200-6400 μm in diameter parallel to the tissue boundary or (2) significantly larger aggregations of deposits; a single cluster often occupying a large area of a gyrus or sector of HC. These results are similar to those reported previously in AD and other disorders [5].

Regular distributed clusters of Aβ deposits along the cortex suggests a spatial relationship with the

neuro-anatomical pathways, especially the cortico-cortical pathways [4]. Hence, the cells of origin of the cortico-cortical projections are clustered and occur in bands which are distributed along the cortex. The individual bands of cells vary in width in the range 400-500 μm up to 800-1000 μm, depending on the cortical region [23]. In a proportion of gyri studied in all disorders, the estimated widths of the clusters of Aβ deposits were within this predicted size range [37]. In the remaining brain regions, clusters of Aβ deposits were significantly larger than 1000 μm. Variation in mean size of the Aβ deposit clusters may depend on disease stage [14,15]. Hence, at an early stage, Aβ deposits may aggregate in smaller clusters associated with specific cortical columns, subsequent Aβ formation resulting in more of the column being affected. Ultimately, the coalescence of the original clusters results in the larger aggregations or more continuous distribution of deposits observed in several regions and disorders.

The observed spatial pattern of the Aβ deposit clusters may be a consequence of the hypothesized 'prion-like' spread of Aβ among regions via neuro-anatomical pathways [20,43]. First, the spatial patterns of the Aβ deposits are similar to those of PrP^{sc} deposits in CJD [7]. Second, in a significant number of regions, regularly distributed clusters of Aβ deposits, 400-800 μm in diameter were present; within the predicted size range of the cell columns associated of the cortico-cortical pathways [16,23,24]. Third, anatomically connected regions exhibited similar regularly distributed clusters of Aβ deposits, e.g., in the adjacent gyri LOT and PHG connected by cortical U-fibers. Fourth, virtually all patients with DS develop Aβ deposits within the brain if they survive into their thirties [30], with particular accumulations of deposits observed between the ages of 30 and 50 years [27]. Cluster sizes of the primitive and classic Aβ deposits in the DS cases increased with age to a maximum in patients aged 45 to 55 and 60 years respectively, declining in size in the oldest patients suggesting growth in size of Aβ deposit clusters at least over part of the age range.

Differences in cluster size of Aβ deposits were also observed among disorders, most notably in CTE which exhibited the smallest-sized clusters of diffuse and primitive deposits. Small cluster size in CTE could be attributable to: (1) lower densities of Aβ deposits overall compared with the other disorders, (2) differences in the vulnerability of anatomical

pathways to the spread of Aβ, a more selective group of neurons being compromised, or (3) differences in the timing and rate of spread of Aβ along neuroanatomical connections, ADNC developing later in CTE compared with the other disorders. Aβ deposits in the form of diffuse and NP have been recorded in 52% and 36% of CTE cases respectively, a frequency which increased with the stage of the disease [42], which lends support to the third hypothesis. By contrast, the classic Aβ deposits in CTE are similar in size to those of the other disorders which may result from specific damage to cerebral microvessels caused by head trauma.

In conclusion, the spatial patterns of the diffuse, primitive, and classic Aβ deposits show considerable similarities in the five disorders studied consistent with the neuro-anatomical spread of Aβ as a common process regardless of clinical or pathological setting.

Acknowledgements

Disclosure

The author reports no conflict of interest.

References

1. Armstrong RA. Quantifying the pathology of neurodegenerative disorders: quantitative measurements, sampling strategies and data analysis. Histopathology 2003; 42: 521-529.
2. Armstrong RA. Methods of studying the planar distribution of objects in histological sections of brain tissue. J Microsc (Oxf) 2006; 221: 153-158.
3. Armstrong RA. A spatial pattern analysis of β-amyloid (Aβ) deposition in the temporal lobe in Alzheimer's disease. Folia Neuropathol 2010; 48: 67-74.
4. Armstrong RA. Evidence from spatial pattern analysis for the anatomical spread of α-synuclein pathology in Parkinson's disease dementia. Folia Neuropathol 2017; 55: 23-30.
5. Armstrong RA, Cairns NJ, Lantos PL. Dementia with Lewy bodies: clustering of Lewy bodies in human patients. Neurosci Lett 1997; 224: 41-44.
6. Armstrong RA, Cairns NJ, Lantos PL. Beta-amyloid deposition in the temporal lobe of patients with dementia with Lewy bodies: Comparison with non-demented cases and Alzheimer's disease. Dement Geriatr Cogn Disord 2000; 11: 187-192.
7. Armstrong RA, Lantos PL, Cairns NJ. The spatial patterns of prion protein deposits in Creutzfeldt-Jacob disease: comparison with β-amyloid deposits in Alzheimer's disease. Neurosci Lett 2001; 298: 53-56.
8. Armstrong RA, Ellis W, Hamilton RL, Mackenzie IRA, Hedreen J, Gearing M, Montine T, Vonsattel J-P, Head E, Lieberman AP, Cairns NJ. Neuropathological heterogeneity in frontotemporal lobar degeneration with TDP-43 proteinopathy: a quantitative study of 94 cases using principal components analysis. J Neural Transm 2010; 117: 227-239.
9. Armstrong RA, McKee AC, Stein TD, Alvarez VE, Cairns NJ. A quantitative study of tau pathology in 11 cases of chronic traumatic encephalopathy. Neuropathol Appl Neurobiol 2016; 43: 154-166.
10. Beekes M, McBride, PA, Baldauf E. Cerebral targeting indicates vagal spread of infection in hamsters fed with scrapie. J Gen Virol 1998; 79: 601-607.
11. Beekes M, McBride PA. Early accumulation of pathological prion protein in the enteric nervous system and gut-associated lymphoid tissue of hamsters orally infected with scrapie. Neurosci Lett 2000; 278: 181-184.
12. Beekes M, Thomzig A, Schultz-Schaeffer W, Burger R. Is there a risk of prion-like transmission by Alzheimer- or Parkinson-associated protein particles? Acta Neuropathol 2014; 128: 463-476.
13. Bland JM, Altman DG. Statistical method for assessing agreement between two methods of clinical measurement. Lancet 1986; 1: 307-310.
14. Braak H, Braak E. The human entorhinal cortex: normal morphology and lamina-specific pathology in various diseases. Neurosci Res 1992; 15: 6-31.
15. Braak H, Braak E, Bohl J. Staging of Alzheimer-related cortical destruction. Eur Neurol 1993; 33: 403-408.
16. De Lacoste M, White CL. The role of cortical connectivity in Alzheimer's disease pathogenesis: a review and model system. Neurobiol Aging 1993; 14: 1-16.
17. Delaere P, Duyckaerts C, He Y, Piette F, Hauw JJ. Subtypes and differential laminar distribution of β/A4 deposits in Alzheimer's disease: Relationship with the intellectual status of 26 cases. Acta Neuropathol 1991; 81: 328-335.
18. Geddes J, Vowles G, Nicoll J, Revesz T. Neuronal cytoskeletal changes are an early consequence of repetitive brain injury. Acta Neuropathol 1999; 98: 171-178.
19. Glenner GG, Wong CW. Alzheimer's disease and Down's syndrome: sharing of a unique cerebrovascular amyloid fibril protein. Biochem Biophys Res Commun 1984; 122: 1131-1135.
20. Goedert M, Clavaguera F, Tolnay M. The propagation of prion-like protein inclusions in neurodegenerative diseases. Trends Neurosci 2010; 33: 317-325.
21. Greenberg BD. The COOH-terminus of the Alzheimer amyloid Aβ peptide: Differences in length influence the process of amyloid deposition in Alzheimer brain, and tell us something about relationships among parenchymal and vessel-asssociated amyloid deposits. Amyloid 1995; 21: 195-203.
22. Hamilton RL, Bouser R. Alzheimer's disease pathology in amyotrophic lateral sclerosis. Acta Neuropathol 2004; 107: 515-522.

23. Hiorns RW, Neal JW, Pearson RCA, Powell TPS. Clustering of ipsilateral cortico-cortical projection neurons to area 7 in the rhesus monkey. Proc Roy Soc (Lond) 1991; 246: 1-9.

24. Holmes BB, Devos SL, Kfoury N, Li M, Jacks R, Yanamandra K, Ouidja MO, Brodsky FM, Marasa J, Bagchi DP, Kotzbauer PT, Miller TM, Papy-Garcia D, Diamond MI. Heparan sulfate proteoglycans mediate internalization and propagation of specific proteopathic seeds. Proc Natl Acad Sci USA 2013; 110: E3138-E3147.

25. Huse JT, Doms RW. Closing in on the amyloid cascade: recent insights into the cell biology of Alzheimer's disease. Mole Neurobiol 2000; 22: 81-98.

26. Hyman BT, West HL, Rebeck GW, Buldyrev RN, Mantegna M, Ukleja M, Harlin S, Stanley HE. Quantitative analysis of senile plaques in Alzheimer's disease: observation of log-normal size distributions associated with apolipoprotein E genotype and trisomy 21 (Down's syndrome). Proc Natl Acad Sci USA 1995; 92: 3586-3590.

27. Hyman BT, Phelps CH, Beach TG, Bigio EH, Cairns NJ, Carrillo MC, Dickson DW, Duyckaerts C, Frosch MP, Masliah E, Mirra SS, Nelson PT, Schneider JA, Thal DR, Thies B, Trojanowski JQ, Vinters HV, Montine TJ. National Institute on Aging-Alzheimer's Association guidelines for the neuropathologic assessment of Alzheimer's disease. Alzheimers Dement 2012; 8: 1-13.

28. Jordan BD. The clinical spectrum of sport-related traumatic brain injury. Nat Rev Neural 2013; 9: 222-230.

29. Lee VMY, Goedert M, Trojanowski JQ. Neurodegenerative tauopathies. Ann Rev Neurosci 2001; 24: 1121-1159.

30. Mann DMA, Esiri MM. The pattern of acquisition of plaques and tangles in the brains of patients under 50 years of age with Down's syndrome. J Neurol Sci 1989; 89: 169-179.

31. McKee AC, Stein TD, Kieman PT, Alvarez VE. The neuropathology of chronic traumatic encephalopathy. Brain Pathol 2015; 25: 350-364.

32. McKee AC, Cairns NJ, Dickson DW, Folkerth RD, Keene CD, Litvan I, Perl D, Stein TD, Vonsattel JP, Stewart W, Tripodis Y, Crary JF, Bienick KF, Dams-O'Connor K, Alverez VF, Gordon WA, the TBI/CTE group. The first NINDS/NIBIB consensus meeting to define neuropathological criteria for the diagnosis of chronic traumatic encephalopathy. Acta Neuropathol 2016; 131: 75-86.

33. McKeith IG, Galasko D, Kosaka K, Perry EK, Dickson DW, Hansen LA, Salmon DP, Lowe J, Mirra SS, Byrne EJ, Lennox G, Quinn NP, Edwardson JA, Ince PG, Bergeron C, Burns A, Miller BL, Lovestone S, Collerton D, Jansen ENH, Ballard C, de Vos RAI, Wilcock GK, Jellinger KA, Perry RH. Consensus guidelines for the clinical and pathological diagnosis of dementia with Lewy bodies (DLB): Report of the consortium on DLB international workshop. Neurology 1996; 47: 1113-1124.

34. Mirra SS, Heyman A, McKeel D, Sumi SM, Crain BJ, Brownlee LM, Vogel FS, Hughes JP, van Belle G, Berg L. The consortium to establish a registry of the neuropathological assessment of Alzheimer's disease (CERAD). II. Standardization of the neuropathological assessment of Alzheimer's disease. Neurology 1991; 41: 479-486.

35. Montine TJ, Phelps CH, Beach TG, Bigio EH, Cairns NJ, Dickson DW, Duyckaerts C, Frosch MP, Masliah E, Mirra SS, Nelson PT, Schneider JA, Thal DR, Trojanowski JQ, Vinters HV, Hyman BT. National Institute on Aging; Alzheimer's Association. National Institute on Aging-Alzheimer's Association guidelines for the neuropathologic assessment of Alzheimer's disease: a practical approach. Acta Neuropathol 2012; 23: 1-11.

36. Motte J, Williams RS. Age-related changes in the density and morphology of plaques and neurofibrillary tangles in Down syndrome brain. Acta Neuropathol 1989; 77: 535-546.

37. Pearson RCA, Esiri MM, Hiorns RW, Wilcock GK, Powell TPS. Anatomical correlates of the distribution of the pathological changes in the neocortex in Alzheimer's disease. Proc Natl Acad Sci USA 1985; 82: 4531-4534.

38. Schneider JA, Watts RL, Gearing M, Brewer RP, Mirra SS. Corticobasal degeneration: neuropathology and clinical heterogeneity. Neurology 1997; 48: 959-969.

39. Selkoe DJ. Deciphering Alzheimer's disease: the amyloid precursor protein yields further new clues. Science 1990; 248: 1058-1060.

40. Spargo E, Luthert PJ, Anderton BH, Bruce M, Smith D, Lantos PL. Antibodies raised against different proteins of A4 protein identify a subset of plaques in Down's syndrome. Neurosci Lett 1990; 115: 345-350.

41. Spillantini MG, Crowther RA, Jakes R, Cairns NJ, Lantos PL, Goedert M. Filamentous α-synuclein inclusions link multiple system atrophy with Parkinson's disease and dementia with Lewy bodies. Neurosci Lett 1998; 251: 205-208.

42. Stein TD, Montenigro PH, Alvarez VE, Xia W, Crary JF, Tripodis Y, Daneshvar DH, Mez J, Soloman T, Meng G, Kubilus CA, Cormier KA, Meng KA, Babcock K, Kiernan P, Murphy L, Nowiski CK, Martin B, Dixon D, Stern RA, Cantu RC, Kowall NW, McKee AC. Beta-amyloid deposition in chronic traumatic encephalopathy. Acta Neuropathol 2015; 130: 21-34.

43. Steiner JA, Angot E, Brunden P. A deadly spread: cellular mechanisms of α-synuclein transfer. Cell Death Differ 2011; 18: 1425-1433.

44. Tierney MC, Fisher RH, Lewis AJ, Zorzitto ML, Snow WG, Reid DW, Nieuwstraten P. The NINCDS-ADRDA work group criteria for the clinical diagnosis of probable Alzheimer's disease. Neurology 1988; 38: 359-364.

45. Wisniewski KE, Wisniewski HM, Wen GY. Occurrence of neuropathological changes and dementia of Alzheimer's disease in Down's syndrome. Ann Neurol 1985; 17: 278-282.